Phonon Monte Carlo Investigation of Hydrodynamic Transport in Graphene Micro Ribbons

Aidan Belanger, and Zlatan Aksamija
Materials Science and Engineering Department, University of Utah,
Salt Lake City, Utah, 84112-0063, USA
e-mail: aidan.belanger@utah.edu

ABSTRACT

Using the Monte Carlo method to solve the Peierls-Boltzmann Transport Equation with boundaries, we simulate thermal transport in graphene micro ribbons. Our phonon dispersion and scattering rates were obtained from first principles with which we explore the interplay between normal, umklapp, and boundary scattering in the hydrodynamic transport regime.

INTRODUCTION

When normal scattering events (momentum conserving) dominate umklapp (momentum reversing) and impurity scattering, the thermal transport becomes hydrodynamic, resembling that of a fluid through a viscous damping term [1]. Graphene has been predicted to have a relatively wide window of temperatures over which hydrodynamic thermal transport can be observed (50-300K) [2]. Although hydrodynamic transport was first demonstrated in the 1960's [4], our capacity to harness this phenomena is only just beginning to be explored. Recently, limited thermal rectification attributed to normal scattering was experimentally demonstrated in a graphite Tesla valve structure [5].

This hydrodynamic transport regime (being non-Fourier) can be accurately modeled through solving the Peierls-Boltzmann Transport Equation (PBTE). Including boundaries when solving the PBTE becomes computationally expensive when using deterministic or iterative techniques [1]. To model the thermal transport in a computationally efficient way, we use the Monte Carlo (MC) simulation method in which phonons are generated from sampling the probability distributions of their energy, momenta and branch polarization and tracked through space [6]. We track phonons in free space and with boundaries (with solely normal and solely umklapp scattering) to examine the influence of boundaries on thermal transport in the hydrodynamic regime.

MODEL

From the interatomic force constants generated by first-principles in VASP [7], we generate a phonon dispersion (see Fig. 1), as well as normal and umklapp phonon scattering rates (see Fig. 2) with the finite displacement supercell approach in Phono3py [8]. With the energy and branch of the phonon assigned through the MC method, the scattering rates are computed by interpolating the lifetime values from Phono3py and dividing those lifetimes by a random number between 0 and 1, to add randomness to the scattering events.

The probability that a phonon is emitted in the scattering process is computed from Fermi's Golden Rule,

$$P(q,q') = \frac{2\pi}{\hbar}|V|^2 n_\lambda \left(n'_\lambda + \frac{1}{2}m\frac{1}{2}\right)(n''_\lambda + 1)\delta_{\pm q+q',q''+G}\,\delta(\omega_\lambda \pm \omega'_\lambda - \omega''_\lambda). \quad (1)$$

In our work, we approximate the delta function in (1) with a lorentzian distribution whose height is inversely proportional to the remaining energy and whose width is determined from the scattering rates of the phonons, $\Gamma'+\Gamma''$, $\delta = \frac{[\hbar(\Gamma'+\Gamma'')]^2}{\hbar^2(\omega_\lambda \pm \omega'^{\prime}_\lambda - \omega''_\lambda)^2 + [\hbar(\Gamma'+\Gamma'')]^2}$. Boundary scattering is treated as either diffusive or specular, using MC sampling of specular probability to determine which scattering event occurs, using the equation, $p_{spec(q)} = e^{-4(\Delta q N)^2}$. The diffusion coefficient is computed at the end of the MC simulation by integrating the velocity autocorrelation, $D = \int_0^\infty \langle V_t V_0 \rangle \, dt$.

The phonon positions after a few nanoseconds of flight time in Fig. 3, and a histogram of their one dimensional travel distances in Fig. 4, show LA and TA phonons with low umklapp scattering rates. Examining the diffusion coefficient in Fig. 5 demonstrates that these modes are responsible for a long transition time between ballistic and diffusive thermal transport. By adding boundaries, the phonon mean free paths are interrupted resulting in a much faster onset of the diffusive transport regime, as shown in Fig. 6.

REFERENCES

[1] M. Raya-Moreno, J. Carrete, and X. Cartoixà, "Hydrodynamic signatures in thermal transport in devices based on two-dimensional materials: An ab initio study," *Phys. Rev. B*, vol. 106, no. 1, p. 014308, Jul. 2022, doi: 10.1103/PhysRevB.106.014308.

[2] S. Lee, D. Broido, K. Esfarjani, and G. Chen, "Hydrodynamic phonon transport in suspended graphene," *Nat. Commun.*, vol. 6, no. 1, Art. no. 1, Feb. 2015, doi: 10.1038/ncomms7290.

[3] K. Ghosh, A. Kusiak, and J.-L. Battaglia, "Phonon hydrodynamics in crystalline materials," *J. Phys. Condens. Matter*, vol. 34, no. 32, p. 323001, Jun. 2022, doi: 10.1088/1361-648X/ac718a.

[4] J. A. Sussmann and A. Thellung, "Thermal Conductivity of Perfect Dielectric Crystals in the Absence of Umklapp Processes," *Proc. Phys. Soc.*, vol. 81, no. 6, p. 1122, Jun. 1963, doi: 10.1088/0370-1328/81/6/318.

[5] X. Huang *et al.*, "A graphite thermal Tesla valve driven by hydrodynamic phonon transport," *Nature*, vol. 634, no. 8036, pp. 1086–1090, Oct. 2024, doi: 10.1038/s41586-024-08052-1.

[6] S. Mei, L. N. Maurer, Z. Aksamija, and I. Knezevic, "Full-dispersion Monte Carlo simulation of phonon transport in micron-sized graphene nanoribbons," *J. Appl. Phys.*, vol. 116, no. 16, p. 164307, Oct. 2014, doi: 10.1063/1.4899235.

[7] J. Hafner, "Ab-initio simulations of materials using VASP: Density-functional theory and beyond," *J. Comput. Chem.*, vol. 29, no. 13, pp. 2044–2078, 2008, doi: 10.1002/jcc.21057.

[8] A. Togo, "First-principles Phonon Calculations with Phonopy and Phono3py," *J. Phys. Soc. Jpn.*, vol. 92, no. 1, p. 012001, Jan. 2023, doi: 10.7566/JPSJ.92.012001.

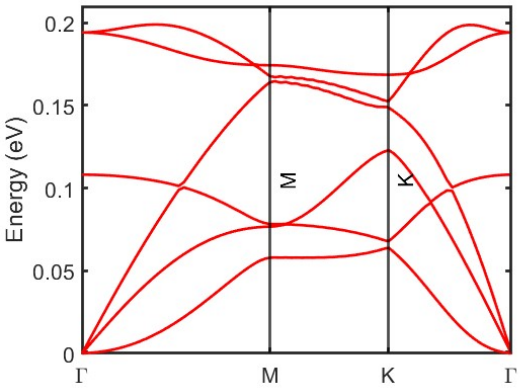

Fig. 1 Phonon dispersion of graphene as generated by Phono3py using a 71x71x1 grid of q points from the force constants of a 5x5x1 supercell of graphene.

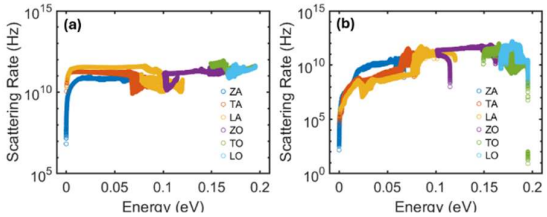

Fig. 2 (a) normal scattering rates and (b) umklapp scattering rates of graphene at 300K interpolated over a dense momentum space using a dataset provided by Phono3py.

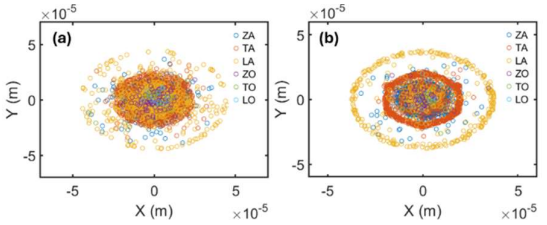

Fig. 3 Phonon positions after random initialization in 1um area and 2 ns of simulation. Implementing (a) normal scattering and (b) umklapp scattering of graphene at 300K.

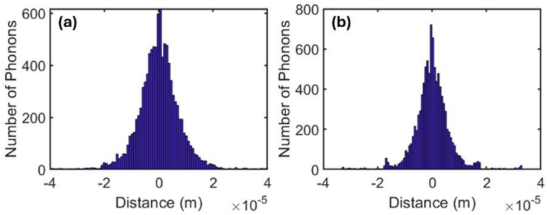

Fig. 4 Histograms of the phonon travel distance along the x direction after random initialization in 1 um area and 2 ns of simulation without boundaries. Implementing (a) normal scattering and (b) umklapp scattering of graphene at 300K.

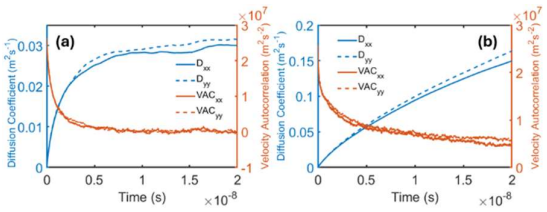

Fig. 5 The diffusion coefficient and its corresponding velocity autocorrelation in the x and y directions over 20 ns with (a) normal and (b) umklapp scattering. No boundaries are enforced in either simulation.

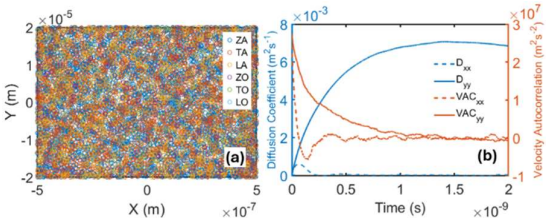

Fig. 6 Using the full scattering rates, (a) the phonon positions in a 1 um by 40 um ribbon after 2 ns of flight time and (b) the diffusion coefficient and velocity autocorrelation in the x and y directions throughout 2 ns of flight time in the ribbon.